

Analysis of Contourlet Texture Feature Extraction to Classify the Benign and Malignant Tumors from Breast Ultrasound Images

Prabhakar Telagarapu¹, Poonguzhali S²

^{1,2}Centre for Medical Electronics, Department of Electronics and Communication, College of Engineering, Guindy, Anna University, Chennai, India, 600025.

¹prabhakart2@gmail.com

²poongs@annauniv.edu

Abstract— The number of Breast cancer has been increasing over the past three decades. Early detection of breast cancer is crucial for an effective treatment. Mammography is used for early detection and screening. Especially for young women, mammography procedures may not be very comfortable. Moreover, it involves ionizing radiation. Ultrasound is broadly popular medical imaging modality because of its non-invasive, real time, convenient and low cost nature. However, the excellence of ultrasound image is corrupted by a speckle noise. The presence of speckle noise severely degrades the signal-to noise ratio (SNR) and contrast resolution of the image. Therefore speckle noise need to be reduced before extracting the features. In this research focus on developing an algorithm to reduce the speckle noise, feature extraction and classification methods for benign and malignant tumors showed that SVM-Polynomial classification produces a high classification rate (77%) for Grey level Co-occurrence matrix (GLCM) based Contourlet features for wavelet soft thresholding denoised breast ultrasound images.

Keyword- Breast, Ultrasound image, Feature extraction, Classification.

I. INTRODUCTION

Breast cancer is the leading cause of death for woman all over the world [1]. Mammography is the most effective modality for detecting and diagnosing the breast cancer [2]. However, there are limitations of mammography in the breast cancer detection especially for young women. It involves ionizing radiation. Ultrasonography has become very popular tool for imaging soft issues in the body because of its non-invasive, real time, convenient and low cost nature. But these images are low contrast and corrupted with noise which is difficult for the Radiologist.

Studies have demonstrated that using ultrasound images can discriminate benign and malignant masses with a high accuracy [3]. At present, there are a number of algorithms for ultrasound images denoising including the Lee [4], Frost Filter [5] and Perona and Malik (PM) [6]. Based on PM, Lee Filter and Frost Filter, Yu and Acton proposed speckle reduction anisotropic diffusion (SRAD) [7] in 2002. SRAD can preserve edges well for ultrasound images when reducing speckle noise in homogenous regions. Several researchers [8] proposed anisotropic diffusion methods based on the original study of Perona and Malik [6], where the anisotropic diffusion equation provides a technique for selective image smoothing. Recently many challenges have been made to reduce the speckle noise using Wavelet Thresholding [9].

Recently, several computer-aided diagnosis (CAD) approaches even have no image pre-processing and image segmentation components, and only extract texture feature for tumor classification [10,11]. The texture feature descriptors are calculated using a variety of statistical, structural, spectral and model based techniques, such as auto-covariance coefficients gray level co-occurrence matrix (GLCM) [12,13], block difference of inverse probabilities, block variation of local correlation coefficients, fractal dimension and complexity curve. These methods can represent the statistical characteristics of gray level distribution in certain region of interest (ROI). However, these methods mainly extract textures feature from the spatial domain, but ignore the frequency domain. Furthermore, most of these methods don't have the multiscale properties of an image. In the past decade, many multiscale geometric analysis (MGA) algorithms have been developed, such as wavelet [14], curvelet [15], contourlet [16, 17]. The classifiers can be grouped as supervised and unsupervised. Most of the recent studies [2] in support vector machine (SVM).

In this paper we focus on first speckle removed by using Mean filter, Median filter, wiener filter, anisotropic diffusion and wavelet thresholding methods. After speckle removal a Region of Interest (ROI) cropped manually. The 21 texture features are extracted from each input breast ultrasound image, anisotropic diffusion

filtered image and wavelet threshold images of benign and malignant tumor by using Contourlet transform with gray level cooccurrence (GLCM) values to classify the breast tumor from ultrasound images. Finally to classified as benign or malignant these features are then fed to the Support machine vector(SVM) with polynomial kernel. The rest of the paper is organized as follows: In section II, we illustrate our data base acquisition, speckle noise reduction methods such as anisotropic diffusion and Wavelet thresholding. Next feature extraction with Contourlet transform based Grey level Co-occurrence matrix (GLCM) and support vector machine classification method. Section III presents the experimental results and the discussion. Finally, Section IV concludes the paper.

II. MATERIAL AND METHODS

A. Data base acquisition

In this study, the Breast ultrasound images are acquired with an ultrasound scanner GE Healthcare LOGIQ E9, using linear transducer array of frequency 5 MHz .The algorithms are applied to sub-images of benign and malignant masses of breast. The dataset consists of 41 cases, of which 15 are benign masses and 26 malignant are solid masses.

B. Speckle noise reduction

Speckle noise removed by using Mean filter, Median filter, wiener filter, anisotropic diffusion and wavelet thresholding methods.

1) Speckle reduction Anisotropic diffusion filter (SRAD): This can preserve edges even enhances edges however this character or function highly depends on the precision of edge detecting. If the edge is not detected, the edge will not be enhanced and even smoothed. And if the noise is detected as edges, the noise will not be smoothed and even enhanced. So the performance of SRAD is sensitive to the selection of threshold value. Although SRAD has a dynamic threshold value, its precision of edge detecting is not so good in experiment. The diffusion coefficient cannot be zero at any edge; hence some edge in the image will be blurred. SRAD is very fit for speckle reducing. SRAD can not only preserve edges but also enhances edges. Given an intensity image having finite power and no zero values over the image, the output image is evolved according to the Partial differential equation [7].

2)Wavelet thresholding: Speckle noise is a high-frequency component of the image and appears in wavelet coefficients. One widespread method exploited for speckle reduction is wavelet soft thresholding procedure [18].

C. Feature extraction

1) Contourlet Transform feature Extraction Method: The Contourlet Transform is a directional multiresolution image representation scheme proposed by Do and Vetterli [19]. The method utilizes a double filter bank, in order to obtain a sparse expansion of typical images containing smooth contours. In this filter bank, first the Laplacian Pyramid (LP) is used to detect the point discontinuities of the image and then a Directional Filter Bank (DFB) to link point discontinuities into linear structures [20].

2) Grey level Co-occurrence matrix (GLCM) based texture features: GLCM matrix based features are well defined and widely used in measuring texture in images. GLCM matrices are two-dimensional histograms. An element of the GLCM matrix $P(i, j, d, \theta)$ is defined as the joint probability of the gray levels i and j separated by distance d and along direction θ . In order to simplify the computational complexity, the value of θ is often given as 0, 45, 90, and 135 degree, and the distance is often defined as the Manhattan distance. The 21 features like Autocorrelation, Contrast, Correlation, Cluster Prominence, Cluster Shade, Dissimilarity, Energy ,Entropy , Inverse difference (INV), Homogeneity , Maximum probability, Sum of squares Variance ,Sum average, Sum variance, Sum entropy, Difference variance, Difference entropy, Information measure of correlation1, Information measure of correlation2 , Inverse difference normalized (INN), Inverse difference moment normalized [21,22,23].

D. Support vector machine (SVM) Classification

SVM tends to find a hyper plane that can separate the input samples. In the case that the original data cannot be separated by a hyper plane, SVM will transform the original data into a feature space of higher dimension by using the kernel function. The popular kernels are Linear kernel, Polynomial kernel of degree 'd', Gaussian radial basis function (RBF), Neural nets (sigmoid). In this work we used Polynomial kernel [24].

III. RESULTS AND DISCUSSION

The developed algorithm results are made on Intel(R) Pentium(R) Dual CPU T2330 1.6 GHz Personal computer with Microsoft Windows operating system.

A. Speckle Reduction

To reduce the speckle noise in breast ultrasound Image we used different filtering techniques like Mean filter, Median filter, wiener filter, anisotropic diffusion and wavelet thresholding methods. The output of the different filters is shown in Fig 1 for Benign and Fig 2 for Malignant. The peak signal to noise ratio (PSNR) is calculated with different filter techniques and shown in Table I. From Table I Anisotropic diffusion filter and Wavelet thresholding filter gives better performance than remaining filters.

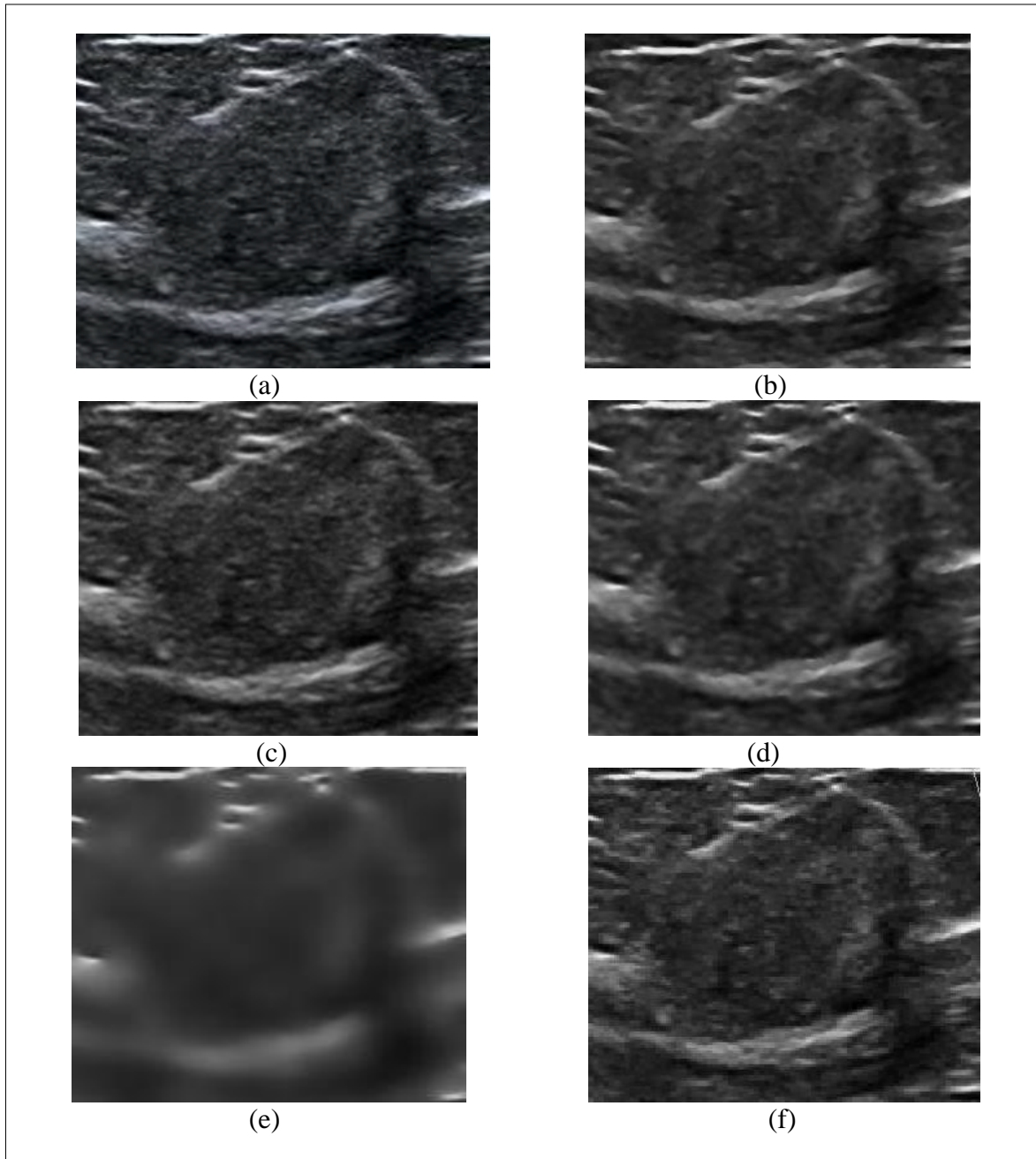


Fig. 1 Speckle noise reduced by several filter techniques for Benign.

(a)The Input image (b) Median filter (c) Mean filter (d) Wiener filter (e) Anisotropic diffusion filter

(f) Wavelet based soft thresholding.

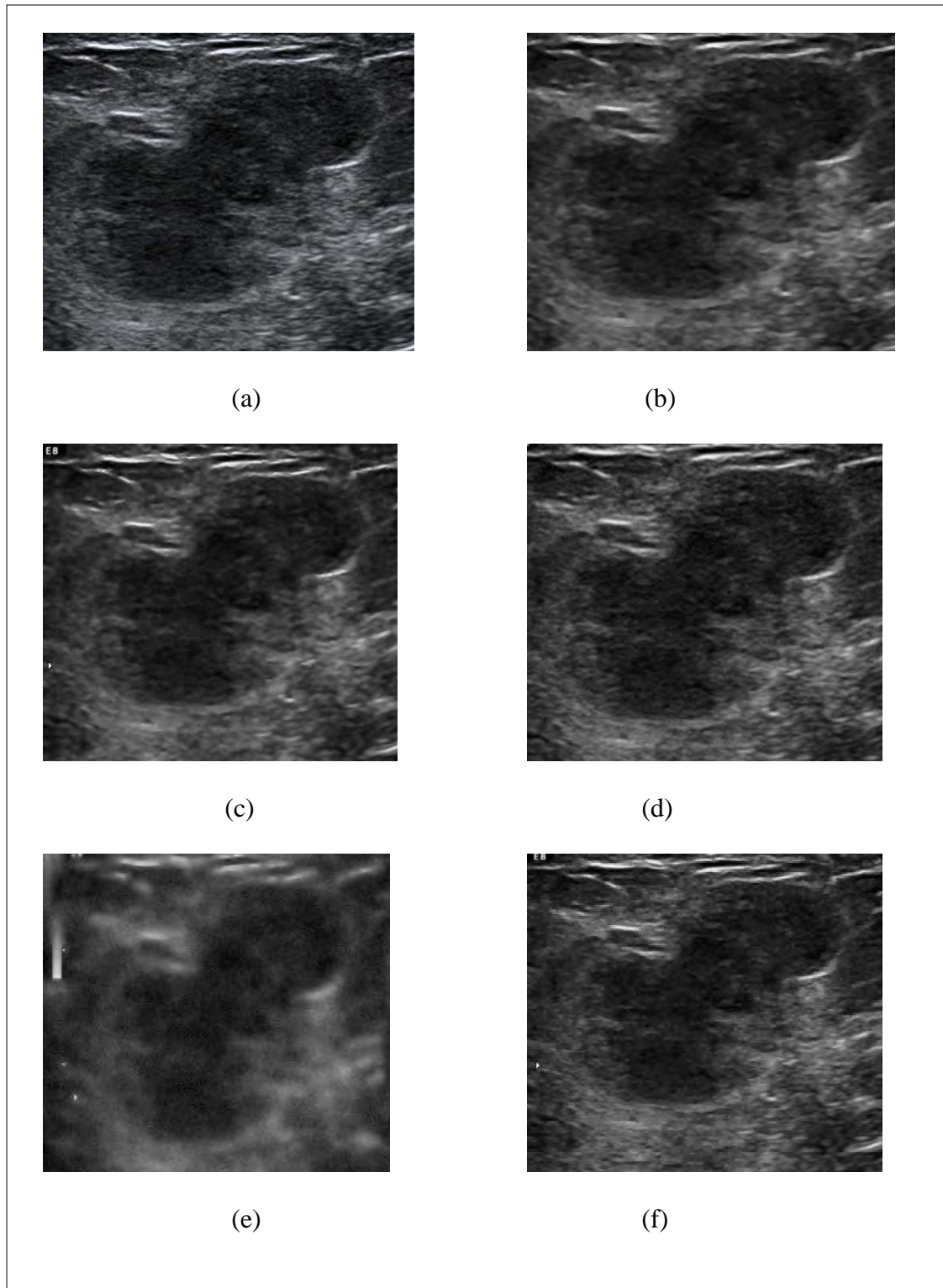


Fig. 2 Speckle noise reduced by several filter techniques for Malignant.

(a) The Input image (b) Median filter (c) Wiener filter (d) Mean filter (e) Anisotropic diffusion filter
(f) Wavelet based soft thresholding.

TABLE I
Comparison of different denoising filters with PSNR for 15 benign and 26 malignant of breast ultrasound images.

Filter	Benign PSNR(dB)		Malignant PSNR(dB)	
	min	max	min	max
Median	21.98	32.60	24.93	37.08
Mean	23.81	36.44	27.80	38.58
Wiener	25.11	36.78	25.58	41.03
Anisotropic Diffusion	69.93	73.41	70.49	74.8
Wavelet soft thresholding	72.14	82.01	75.13	86.3

B. Grey level Co-occurrence matrix (GLCM) based texture features

After speckle noise reduction a Region of Interest (ROI) cropped manually. To select the ROI, the position of mass was roughly located at the centre of the Input breast ultrasound image, and then the image was cropped to the size of 64×64 . The 21 texture features are extracted by using Contourlet transform based on gray level co-occurrence matrix (GLCM). Texture features can be extracted from GLCM matrices with different distances d and directions θ . In practice, given a distance d (1, 2, and 4) four GLCM matrices can be calculated corresponding to 0, 45, 90, and 135 degree, respectively, and produce a set of four values for each of the 21 features, compute the mean and range of the four values. Therefore, a set of 42 textural features is extracted for a given distances d (1, 2, 4). Hence, totally 126 dimensional texture features are extracted from each Input breast ultrasound image, anisotropic diffusion filtered image and wavelet threshold images of benign and malignant. The extracted GLCM based contourlet texture features for the mean, standard deviation and range of benign and malignant with $d=1, 2, 4$ are listed in Table II to VII.

The Table II to VII shows GLCM based contourlet feature extraction for benign and malignant mean, standard deviation and range feature values for $d=1, 2, 4$ and ($\theta=0^\circ, 45^\circ, 90^\circ, 135^\circ$). From Table II to VII observed that benign and malignant of Auto correlation, Contrast, Cluster Prominence, Cluster shade, Sum of squares Variance Sum average and Sum variance and has the highest mean, range and standard deviation values. This characteristic creates a problem for classification.

C. Support vector machine (SVM-Polynomial) Classification

The extracted features are given as input to the classifier such as support vector machine (SVM) to identify benign and malignant tumors from breast ultrasound image. A total of 41 image samples from 15 benign and 26 malignant are considered in which the random set of benign and malignant of 126 features are used as training data set. The random sets of benign and malignant image samples with 126 features are used as testing data set. To estimate the performance of the experimental result, 4 objective indices are used. These indices are accuracy, sensitivity, positive predictive value (PPV), and negative predictive value (NPV).

The indices measures for contourlet feature extraction method with Input image as breast ultrasound, anisotropic diffusion filtered image and wavelet threshold images by using SVM with Polynomial kernel as listed in Table VIII and IX. The Table VIII shows that the false positive rate (FP) is very less for Wavelet soft thresholding contourlet feature extraction than anisotropic diffusion filtered contourlet feature extraction and Input breast ultrasound image contourlet feature extraction. The Table IX shows that the classification accuracy using Wavelet soft thresholding contourlet feature extraction is higher when compared with anisotropic diffusion filtered contourlet feature extraction and Input breast ultrasound image contourlet feature extraction. So the overall SVM performance for Wavelet soft thresholding contourlet feature extraction dominates than anisotropic diffusion filtered contourlet feature extraction and Input breast ultrasound image contourlet feature extraction. Thus, it is clear that the proposed approach can classify benign and malignant.

TABLE II

GLCM Based Contourlet feature extraction for Benign mean, Standard Deviation and Range feature values for $d=1(\theta=0^\circ, 45^\circ, 90^\circ, 135^\circ)$.

S.No	Statistical Measures	Breast ultrasound input Image		Speckle reduction anisotropic diffusion filter image		Wavelet Soft thresholding filter image	
		Mean \pm S.D	Range	Mean \pm S.D	Range	Mean \pm S.D	Range
1	Autocorrelation	22.56 \pm 6.54	25.12	16.01 \pm 3.26	10.29	20.93 \pm 6.74	25.29
2	Contrast	22.86 \pm 2.65	10.17	22.67 \pm 3.03	10.29	24.38 \pm 3.22	13.29
3	Correlation	0.02 \pm 0.07	0.20	-0.04 \pm 0.08	0.26	-0.05 \pm 0.08	0.34
4	Cluster Prominence	1155.83 \pm 74.99	248.28	963.35 \pm 155.61	601.28	1042.04 \pm 69.14	219.42
5	Cluster Shade	-9.42 \pm 29.10	99.47	16.24 \pm 16.23	55.41	-7.20 \pm 26.94	104.49
6	Dissimilarity	3.33 \pm 0.35	1.35	3.48 \pm 0.33	1.02	3.59 \pm 0.45	1.88
7	Energy	0.26 \pm 0.04	0.17	0.20 \pm 0.05	0.14	0.24 \pm 0.04	0.16
8	Entropy	1.48 \pm 0.16	0.51	1.90 \pm 0.37	1.07	1.61 \pm 0.15	0.53
9	Inverse difference	0.57 \pm 0.04	0.16	0.51 \pm 0.04	0.15	0.53 \pm 0.06	0.22
10	Homogeneity	0.52 \pm 0.04	0.18	0.45 \pm 0.05	0.18	0.47 \pm 0.06	0.25
11	Maximum probability	0.33 \pm 0.07	0.28	0.30 \pm 0.03	0.12	0.31 \pm 0.07	0.30
12	Sum of squares Variance	33.83 \pm 5.30	20.30	27.09 \pm 4.26	14.51	33.23 \pm 5.35	18.87
13	Sum average	9.38 \pm 1.22	4.59	8.07 \pm 0.83	2.65	9.22 \pm 1.17	4.31
14	Sum variance	92.67 \pm 20.42	78.21	64.99 \pm 16.28	48.90	86.57 \pm 21.85	77.75
15	Sum entropy	1.15 \pm 0.16	0.52	1.52 \pm 0.36	1.04	1.26 \pm 0.14	0.54
16	Difference variance	22.86 \pm 2.65	10.17	22.67 \pm 3.03	10.29	24.38 \pm 3.22	13.29
17	Difference entropy	0.84 \pm 0.17	0.57	1.21 \pm 0.34	0.95	0.97 \pm 0.15	0.56
18	Information Measure of correlation1	-0.05 \pm 0.03	0.09	-0.15 \pm 0.06	0.19	-0.08 \pm 0.03	0.12
19	Information Measure of correlation2	0.25 \pm 0.10	0.30	0.49 \pm 0.15	0.48	0.34 \pm 0.09	0.35
20	Inverse Difference normalized	0.78 \pm 0.02	0.09	0.76 \pm 0.02	0.06	0.76 \pm 0.03	0.12
21	Inverse Difference moment normalized	0.80 \pm 0.02	0.09	0.79 \pm 0.02	0.08	0.78 \pm 0.03	0.12

TABLE III

GLCM Based Contourlet feature extraction for Malignant mean, Standard Deviation and Range feature values for $d=1(\theta=0^\circ, 45^\circ, 90^\circ, 135^\circ)$.

S.No	Statistical Measures	Breast ultrasound input Image		Speckle reduction anisotropic diffusion filtered image		Wavelet Soft thresholding filtered image	
		Mean \pm S.D	Range	Mean \pm S.D	Range	Mean \pm S.D	Range
1	Autocorrelation	19.35 \pm 3.62	13.38	16.12 \pm 3.46	12.63	19.27 \pm 3.05	10.92
2	Contrast	25.07 \pm 1.62	7.54	24.28 \pm 3.08	12.82	25.85 \pm 1.64	6.60
3	Correlation	-0.05 \pm 0.06	0.26	-0.10 \pm 0.08	0.33	-0.08 \pm 0.06	0.22
4	Cluster Prominence	1100.95 \pm 69.44	238.69	888.95 \pm 141.05	529.20	1048.04 \pm 64.95	226.74
5	Cluster Shade	1.69 \pm 16.28	61.21	10.07 \pm 13.55	57.73	1.92 \pm 12.59	53.37
6	Dissimilarity	3.63 \pm 0.22	1.01	3.71 \pm 0.32	1.45	3.76 \pm 0.21	0.78
7	Energy	0.25 \pm 0.02	0.07	0.21 \pm 0.05	0.19	0.24 \pm 0.02	0.07
8	Entropy	1.48 \pm 0.13	0.45	1.87 \pm 0.39	1.34	1.54 \pm 0.12	0.47
9	Inverse difference	0.54 \pm 0.03	0.11	0.48 \pm 0.04	0.13	0.51 \pm 0.03	0.09
10	Homogeneity	0.48 \pm 0.03	0.12	0.41 \pm 0.05	0.15	0.46 \pm 0.03	0.10
11	Maximum probability	0.31 \pm 0.02	0.10	0.30 \pm 0.04	0.17	0.30 \pm 0.02	0.08
12	Sum of squares Variance	31.57 \pm 3.36	12.99	28.11 \pm 4.32	16.55	31.79 \pm 2.79	10.44
13	Sum average	8.90 \pm 0.74	2.61	8.27 \pm 0.86	3.38	8.92 \pm 0.62	2.30
14	Sum variance	83.61 \pm 11.42	44.01	66.91 \pm 15.21	56.67	82.34 \pm 10.25	38.55
15	Sum entropy	1.13 \pm 0.14	0.48	1.47 \pm 0.36	1.25	1.17 \pm 0.13	0.52
16	Difference variance	25.07 \pm 1.62	7.54	24.28 \pm 3.08	12.82	25.85 \pm 1.64	6.60
17	Difference entropy	0.82 \pm 0.14	0.46	1.19 \pm 0.34	1.18	0.87 \pm 0.13	0.48
18	Information Measure of correlation1	-0.05 \pm 0.03	0.12	-0.16 \pm 0.06	0.26	-0.08 \pm 0.03	0.11
19	Information Measure of correlation2	0.25 \pm 0.11	0.39	0.51 \pm 0.15	0.54	0.33 \pm 0.08	0.34
20	Inverse Difference normalized	0.76 \pm 0.01	0.06	0.74 \pm 0.02	0.08	0.75 \pm 0.01	0.05
21	Inverse Difference moment normalized	0.78 \pm 0.01	0.06	0.78 \pm 0.02	0.10	0.77 \pm 0.01	0.05

TABLE IV

GLCM Based Contourlet feature extraction for Benign Mean, Standard Deviation and Range feature values for $d=2(\theta=0^\circ, 45^\circ, 90^\circ, 135^\circ)$.

S.No	Statistical Measures	Breast ultrasound input Image		Speckle reduction anisotropic diffusion filter image		Wavelet Soft thresholding filter image	
		Mean \pm S.D	Range	Mean \pm S.D	Range	Mean \pm S.D	Range
1	Autocorrelation	21.61 \pm 6.79	27.41	16.70 \pm 3.34	10.09	20.52 \pm 6.72	26.16
2	Contrast	24.53 \pm 2.90	13.50	21.44 \pm 3.04	9.02	24.99 \pm 2.65	11.00
3	Correlation	-0.05 \pm 0.07	0.27	0.03 \pm 0.08	0.24	-0.08 \pm 0.06	0.23
4	Cluster Prominence	1060.65 \pm 107.29	337.87	1042.02 \pm 151.01	462.99	992.62 \pm 109.46	427.61
5	Cluster Shade	-6.75 \pm 23.42	91.07	21.12 \pm 18.85	62.60	-3.04 \pm 18.91	72.48
6	Dissimilarity	3.55 \pm 0.40	1.83	3.29 \pm 0.33	0.97	3.67 \pm 0.36	1.52
7	Energy	0.26 \pm 0.04	0.20	0.20 \pm 0.04	0.13	0.24 \pm 0.04	0.16
8	Entropy	1.44 \pm 0.13	0.53	1.85 \pm 0.33	0.94	1.57 \pm 0.15	0.49
9	Inverse difference	0.55 \pm 0.05	0.21	0.54 \pm 0.04	0.14	0.52 \pm 0.04	0.18
10	Homogeneity	0.49 \pm 0.05	0.23	0.48 \pm 0.05	0.16	0.46 \pm 0.05	0.20
11	Maximum probability	0.34 \pm 0.07	0.32	0.30 \pm 0.04	0.15	0.31 \pm 0.07	0.28
12	Sum of squares Variance	33.62 \pm 6.06	22.21	27.22 \pm 4.73	16.71	33.06 \pm 5.98	21.28
13	Sum average	9.35 \pm 1.28	4.99	8.07 \pm 0.89	2.89	9.20 \pm 1.26	4.85
14	Sum variance	91.61 \pm 22.00	87.75	66.53 \pm 16.92	50.65	86.34 \pm 23.04	87.06
15	Sum entropy	1.10 \pm 0.13	0.48	1.52 \pm 0.33	0.97	1.22 \pm 0.15	0.51
16	Difference variance	24.53 \pm 2.90	13.50	21.44 \pm 3.04	9.02	24.99 \pm 2.65	11.00
17	Difference entropy	0.81 \pm 0.13	0.47	1.20 \pm 0.34	0.96	0.94 \pm 0.14	0.52
18	Information Measure of correlation1	-0.05 \pm 0.03	0.09	-0.12 \pm 0.06	0.17	-0.07 \pm 0.04	0.16
19	Information Measure of correlation2	0.26 \pm 0.09	0.33	0.44 \pm 0.16	0.47	0.33 \pm 0.11	0.41
20	Inverse Difference normalized	0.76 \pm 0.03	0.12	0.77 \pm 0.02	0.06	0.75 \pm 0.02	0.10
21	Inverse Difference moment normalized	0.78 \pm 0.03	0.12	0.80 \pm 0.02	0.07	0.78 \pm 0.02	0.10

TABLE V

GLCM Based Contourlet feature extraction for Malignant mean, Standard Deviation and Range feature values for $d=2(\theta=0^\circ, 45^\circ, 90^\circ, 135^\circ)$.

S.No	Statistical Measures	Breast ultrasound input Image		Speckle reduction anisotropic diffusion filtered image		Wavelet Soft thresholding filtered image	
		Mean \pm S.D	Range	Mean \pm S.D	Range	Mean \pm S.D	Range
1	Autocorrelation	19.87 \pm 3.56	13.71	17.55 \pm 4.02	16.39	19.57 \pm 2.96	10.80
2	Contrast	24.60 \pm 1.70	7.40	22.19 \pm 2.73	11.00	24.67 \pm 2.09	7.66
3	Correlation	-0.03 \pm 0.07	0.32	-0.01 \pm 0.09	0.32	-0.03 \pm 0.09	0.31
4	Cluster Prominence	1121.06 \pm 104.52	459.09	982.25 \pm 179.00	750.91	1105.07 \pm 110.87	416.97
5	Cluster Shade	0.62 \pm 16.38	61.65	10.33 \pm 15.62	57.47	1.33 \pm 12.40	55.52
6	Dissimilarity	3.56 \pm 0.25	1.06	3.43 \pm 0.29	1.03	3.59 \pm 0.29	1.09
7	Energy	0.25 \pm 0.02	0.10	0.20 \pm 0.05	0.17	0.24 \pm 0.02	0.07
8	Entropy	1.47 \pm 0.14	0.51	1.89 \pm 0.38	1.34	1.53 \pm 0.12	0.47
9	Inverse difference	0.54 \pm 0.03	0.14	0.51 \pm 0.05	0.19	0.54 \pm 0.04	0.15
10	Homogeneity	0.49 \pm 0.04	0.16	0.45 \pm 0.06	0.21	0.48 \pm 0.04	0.17
11	Maximum probability	0.31 \pm 0.03	0.13	0.29 \pm 0.05	0.17	0.30 \pm 0.02	0.09
12	Sum of squares Variance	31.53 \pm 3.54	13.71	28.37 \pm 4.27	18.37	31.53 \pm 2.84	10.94
13	Sum average	8.96 \pm 0.75	2.73	8.36 \pm 0.92	4.00	8.92 \pm 0.61	2.29
14	Sum variance	85.06 \pm 11.52	43.67	69.44 \pm 16.47	67.48	83.39 \pm 10.49	37.47
15	Sum entropy	1.13 \pm 0.14	0.57	1.53 \pm 0.35	1.23	1.18 \pm 0.12	0.54
16	Difference variance	24.60 \pm 1.70	7.40	22.19 \pm 2.73	11.00	24.67 \pm 2.09	7.66
17	Difference entropy	0.81 \pm 0.15	0.52	1.22 \pm 0.34	1.15	0.87 \pm 0.12	0.48
18	Information Measure of correlation1	-0.05 \pm 0.03	0.14	-0.14 \pm 0.07	0.23	-0.07 \pm 0.03	0.11
19	Information Measure of correlation2	0.25 \pm 0.11	0.45	0.48 \pm 0.16	0.55	0.32 \pm 0.08	0.33
20	Inverse Difference normalized	0.76 \pm 0.02	0.07	0.76 \pm 0.02	0.08	0.76 \pm 0.02	0.07
21	Inverse Difference moment normalized	0.78 \pm 0.02	0.07	0.80 \pm 0.02	0.08	0.78 \pm 0.02	0.07

TABLE VI

GLCM Based Contourlet feature extraction for Benign mean, Standard Deviation and Range feature values for $d=4(\theta=0^\circ, 45^\circ, 90^\circ, 135^\circ)$.

S.No	Statistical Measures	Breast ultrasound input Image		Speckle reduction anisotropic diffusion filter image		Wavelet Soft thresholding filter image	
		Mean \pm S.D	Range	Mean \pm S.D	Range	Mean \pm S.D	Range
1	Autocorrelation	21.84 ± 4.93	17.53	15.26 ± 3.15	11.58	20.44 ± 5.71	21.70
2	Contrast	24.02 ± 2.49	9.86	24.83 ± 3.01	9.61	25.06 ± 3.12	11.48
3	Correlation	-0.01 ± 0.11	0.41	-0.13 ± 0.10	0.35	-0.07 ± 0.13	0.47
4	Cluster Prominence	1061.86 ± 208.64	815.39	816.67 ± 186.10	631.14	988.11 ± 189.41	598.82
5	Cluster Shade	-2.79 ± 19.77	71.91	11.25 ± 12.74	48.48	-4.05 ± 18.62	65.46
6	Dissimilarity	3.49 ± 0.36	1.45	3.79 ± 0.32	1.19	3.68 ± 0.46	1.58
7	Energy	0.28 ± 0.03	0.10	0.22 ± 0.05	0.14	0.25 ± 0.02	0.09
8	Entropy	1.40 ± 0.11	0.37	1.71 ± 0.29	0.80	1.50 ± 0.10	0.33
9	Inverse difference	0.55 ± 0.05	0.19	0.47 ± 0.05	0.16	0.52 ± 0.06	0.19
10	Homogeneity	0.50 ± 0.05	0.22	0.40 ± 0.05	0.19	0.46 ± 0.07	0.21
11	Maximum probability	0.37 ± 0.04	0.13	0.32 ± 0.04	0.15	0.34 ± 0.04	0.16
12	Sum of squares Variance	33.13 ± 6.37	21.65	27.44 ± 5.02	20.54	32.57 ± 5.76	18.89
13	Sum average	9.34 ± 1.14	4.19	8.13 ± 0.85	3.19	9.18 ± 1.06	3.94
14	Sum variance	92.08 ± 16.98	60.39	65.83 ± 16.67	58.32	86.72 ± 18.90	65.50
15	Sum entropy	1.10 ± 0.12	0.46	1.38 ± 0.31	0.84	1.17 ± 0.10	0.33
16	Difference variance	24.02 ± 2.49	9.86	24.83 ± 3.01	9.61	25.06 ± 3.12	11.48
17	Difference entropy	0.80 ± 0.14	0.43	1.14 ± 0.33	1.00	0.90 ± 0.11	0.41
18	Information Measure of correlation1	-0.06 ± 0.04	0.14	-0.17 ± 0.08	0.26	-0.10 ± 0.05	0.20
19	Information Measure of correlation2	0.27 ± 0.10	0.39	0.51 ± 0.16	0.54	0.36 ± 0.10	0.41
20	Inverse Difference normalized	0.77 ± 0.02	0.10	0.74 ± 0.02	0.07	0.75 ± 0.03	0.10
21	Inverse Difference moment normalized	0.79 ± 0.02	0.09	0.77 ± 0.02	0.08	0.78 ± 0.03	0.10

TABLE VII

GLCM Based Contourlet feature extraction for Malignant mean, Standard Deviation and Range feature values for $d=4(\theta=0^\circ, 45^\circ, 90^\circ, 135^\circ)$.

S.No	Statistical Measures	Breast ultrasound input Image		Speckle reduction anisotropic diffusion filtered image		Wavelet Soft thresholding filtered image	
		Mean \pm S.D	Range	Mean \pm S.D	Range	Mean \pm S.D	Range
1	Autocorrelation	19.53 \pm 3.12	13.21	17.02 \pm 3.07	12.06	19.59 \pm 2.44	8.23
2	Contrast	25.6 \pm 0.13	13.00	23.81 \pm 3.98	15.75	24.63 \pm 3.36	13.89
3	Correlation	-0.07 \pm 0.13	0.53	-0.07 \pm 0.14	0.61	-0.03 \pm 0.13	0.57
4	Cluster Prominence	1046.39 \pm 11.75	683.68	945.04 \pm 190.31	588.62	1095.02 \pm 170.65	696.10
5	Cluster Shade	0.59 \pm 0.43	47.71	11.66 \pm 17.68	86.38	2.06 \pm 12.74	52.43
6	Dissimilarity	3.70 \pm 0.02	1.81	3.63 \pm 0.50	2.03	3.58 \pm 0.47	1.98
7	Energy	0.27 \pm 0.11	0.07	0.23 \pm 0.06	0.24	0.26 \pm 0.02	0.09
8	Entropy	1.41 \pm 0.05	0.39	1.70 \pm 0.31	1.23	1.45 \pm 0.10	0.38
9	Inverse difference	0.53 \pm 0.06	0.22	0.49 \pm 0.07	0.25	0.54 \pm 0.06	0.25
10	Homogeneity	0.47 \pm 0.03	0.25	0.43 \pm 0.07	0.28	0.48 \pm 0.07	0.28
11	Maximum probability	0.35 \pm 4.00	0.10	0.32 \pm 0.06	0.23	0.34 \pm 0.03	0.10
12	Sum of squares Variance	31.52 \pm 0.73	16.00	28.42 \pm 3.81	16.42	31.29 \pm 3.38	15.61
13	Sum average	9.00 \pm 11.58	2.66	8.40 \pm 0.79	3.16	8.92 \pm 0.54	1.88
14	Sum variance	85.48 \pm 0.14	44.23	70.96 \pm 13.57	49.89	84.14 \pm 8.38	28.00
15	Sum entropy	1.08 \pm 3.12	0.56	1.37 \pm 0.33	1.30	1.13 \pm 0.14	0.50
16	Difference variance	25.60 \pm 0.13	13.00	23.81 \pm 3.98	15.75	24.63 \pm 3.36	13.89
17	Difference entropy	0.78 \pm 0.05	0.49	1.09 \pm 0.32	1.23	0.82 \pm 0.13	0.48
18	Information Measure of correlation1	-0.08 \pm 0.12	0.22	-0.18 \pm 0.10	0.39	-0.10 \pm 0.04	0.21
19	Information Measure of correlation2	0.29 \pm 0.03	0.48	0.51 \pm 0.16	0.61	0.35 \pm 0.07	0.26
20	Inverse Difference normalized	0.75 \pm 0.03	0.12	0.75 \pm 0.03	0.13	0.76 \pm 0.03	0.13
21	Inverse Difference moment normalized	0.77 \pm 5.01	0.11	0.78 \pm 0.03	0.13	0.78 \pm 0.03	0.12

Table VIII

Classification of breast tumor by SVM-Polynomial classification with GLCM based Contourlet features with different denoised features

	Breast ultrasound Image		
	Input Image (without filter)	Filtered Images	
		Anisotropic diffusion	Wavelet soft thresholding
True Positive (TP)	25	23	25
True Negative (TN)	2	6	8
False Positive (FP)	13	9	7
False Negative (FN)	1	3	2

TP-Malignant as Malignant

FN-Malignant as Benign

TN-Benign as Benign

FP-Benign as Malignant

Table IX

Indices result by SVM-Polynomial classification with GLCM based Contourlet features with different denoised features.

Index	Input Image (without filter)	SRAD filter Image	Wavelet Thresholding filter Image
Accuracy	66%	71%	77%
Sensitivity	96%	88%	93%
PPV	66%	71%	78%
NPV	67%	66%	80%

Accuracy = $(TP+TN) / (TP+TN+FP+FN)$ Sensitivity = $TP / (TP+FN)$ Positive Predictive Value = $TP / (TP+FP)$ Negative Predictive Value = $TN / (TN+FN)$

IV. CONCLUSION

The proposed Wavelet soft thresholding contourlet feature extraction technique with SVM polynomial kernel classification produces a high classification rate (77%). The features are extracted and given to the support vector machine (SVM) classifier. In SVM we used polynomial kernel. The classification performance of Wavelet soft thresholding contourlet feature extraction gives better result than Input image contourlet features and anisotropic diffusion filter features. In future, if the optimal features are selected then the performance of the classifier may be improved for better diagnosis. Therefore the proposed approach could be helpful in detecting the breast cancer more accurately.

ACKNOWLEDGMENT

We would like to thank Bharat Scans, Royapettah, Chennai, for providing breast ultrasound images and clinical information.

REFERENCES

- [1] Siegel, Rebecca, Deepa Naishadham, and Ahmedin Jemal. "Cancer statistics, 2013." CA: a cancer journal for clinicians 63, no. 1 (2013): 11-30.
- [2] Cheng, H. D., Juan Shan, Wen Ju, Yanhui Guo, and Ling Zhang. "Automated breast cancer detection and classification using ultrasound images: A survey." Pattern Recognition 43, no. 1 (2010): 299-317.
- [3] Shi, Xiangjun, H. D. Cheng, Liming Hu, Wen Ju, and Jiawei Tian. "Detection and classification of masses in breast ultrasound images." Digital Signal Processing 20, no. 3 (2010): 824-836.
- [4] Lee, Jong-Sen. "Digital image enhancement and noise filtering by use of local statistics." Pattern Analysis and Machine Intelligence, IEEE Transactions on 2 (1980): 165-168.
- [5] Frost, Victor S., et al. "A model for radar images and its application to adaptive digital filtering of multiplicative noise." Pattern Analysis and Machine Intelligence, IEEE Transactions on 2 (1982): 157-166.
- [6] Perona, Pietro, and Jitendra Malik. "Scale-space and edge detection using anisotropic diffusion." Pattern Analysis and Machine Intelligence, IEEE Transactions on 12.7 (1990): 629-639.
- [7] Yu, Yongjian, and Scott T. Acton. "Speckle reducing anisotropic diffusion." Image Processing, IEEE Transactions on 11.11 (2002): 1260-1270.
- [8] Liu, Shen, et al. "An anisotropic diffusion filter for reducing speckle noise of ultrasound images based on separability." Signal & Information Processing Association Annual Summit and Conference (APSIPA ASC), 2012 Asia-Pacific. IEEE, 2012.
- [9] Sudha, S., G. R. Suresh, and R. Sukanesh. "Speckle noise reduction in ultrasound images by wavelet thresholding based on weighted variance." International journal of computer theory and engineering 1.1 (2009): 1793-8201.
- [10] Chen, Dar-Ren, et al. "Diagnosis of breast tumors with sonographic texture analysis using wavelet transform and neural networks." Ultrasound in medicine & biology 28.10 (2002): 1301-1310.
- [11] Chen, Dar-Ren, Yu-Len Huang, and Sheng-Hsiung Lin. "Computer-aided diagnosis with textural features for breast lesions in sonograms." Computerized Medical Imaging and Graphics 35.3 (2011): 220-226.

- [12] Poonguzhali, S., B. Deepalakshmi, and G. Ravindran. "Optimal feature selection and automatic classification of abnormal masses in ultrasound liver images." *Signal Processing, Communications and Networking*, 2007. ICSCN'07. International Conference on. IEEE, 2007.
- [13] Alvarenga, André Victor, et al. "Complexity curve and grey level co-occurrence matrix in the texture evaluation of breast tumor on ultrasound images." *Medical physics* 34 (2007): 379.
- [14] B.Balasuganya, Telagarapu Prabhakar and S.Poonguzhali "An Evaluation of Different Feature Extraction Methods for Classification of Tumor in Breast Ultrasound Images" *International Conference on Computation of Power, Energy, Information and Communication (ICPEIC-2013)*, 2013.
- [15] Dettori, Lucia, and Lindsay Semler. "A comparison of wavelet, ridgelet, and curvelet-based texture classification algorithms in computed tomography." *Computers in Biology and Medicine* 37.4 (2007): 486-498.
- [16] Katsigiannis, Stamos, Eystratios G. Keramidas, and Dimitris Maroulis. "A contourlet transform feature extraction scheme for ultrasound thyroid texture classification." *International Journ Engineering Intelligent Systems Electrical Engineering Communications* 18.3 (2010): 171.
- [17] Swaminathan, Anand, Shantha Selva Kumari Ramapackiam, Thivya Thiraviam, and Jeeva Selvaraj. "Contourlet transform-based sharpening enhancement of retinal images and vessel extraction application." *Biomedizinische Technik/Biomedical Engineering* 58, no. 1 (2013): 87-96.
- [18] Donoho, David L., and Iain M. Johnstone. "Adapting to unknown smoothness via wavelet shrinkage." *Journal of the american statistical association* 90.432 (1995): 1200-1224.
- [19] Do, Minh N., and Martin Vetterli. "Contourlets: a directional multiresolution image representation." *Image Processing. 2002. Proceedings. 2002 International Conference on. Vol. 1. IEEE, 2002.*
- [20] Do MN, Vetterli M. The contourlet transform: an efficient directional multiresolution image representation. *IEEE Transactions on Image Processing.* 2005; 14(12): 2091- 106
- [21] Haralick, Robert M., Karthikeyan Shanmugam, and Its' Hak Dinstein. "Textural features for image classification." *Systems, Man and Cybernetics, IEEE Transactions on* 6 (1973): 610-621.
- [22] Soh, L.-K., and Costas Tsatsoulis. "Texture analysis of SAR sea ice imagery using gray level co-occurrence matrices." *Geoscience and Remote Sensing, IEEE Transactions on* 37.2 (1999): 780-795.
- [23] Clausi, David A. "An analysis of co-occurrence texture statistics as a function of grey level quantization." *Canadian Journal of remote sensing* 28.1 (2002): 45-62.
- [24] Vapnik, Vladimir. *The nature of statistical learning theory.* springer, 2000.